Dangling Bonds in Hexagonal Boron Nitride as Single-Photon Emitters

Mark E. Turiansky, Audrius Alkauskas, Lee C. Bassett, and Chris G. Van de Walle

Phys. Rev. Lett. **123**, 127401 — Published 16 September 2019

DOI: 10.1103/PhysRevLett.123.127401

Dangling Bonds in Hexagonal Boron Nitride as Single-Photon Emitters

Mark E. Turiansky[1], Audrius Alkauskas[2], Lee C. Bassett[3], and Chris G. Van de Walle[4]
[1] *Department of Physics, University of California, Santa Barbara, CA 93106-9530, U.S.A.*
[2] *Center for Physical Sciences and Technology (FTMC), Vilnius LT-10257, Lithuania*
[3] *Quantum Engineering Laboratory, Department of Electrical and Systems Engineering, University of Pennsylvania, Philadelphia, PA 19104, U.S.A. and*
[4] *Materials Department, University of California, Santa Barbara, CA 93106-5050, U.S.A.*
(Dated: July 10, 2019)

Hexagonal boron nitride has been found to host color centers that exhibit single-photon emission, but the microscopic origin of these emitters is unknown. We propose boron dangling bonds as the likely source of the observed single-photon emission around 2 eV. An optical transition where an electron is excited from a doubly-occupied boron dangling bond to a localized B p_z state gives rise to a zero-phonon line of 2.06 eV and emission with a Huang-Rhys factor of 2.3. This transition is linearly polarized with the absorptive and emissive dipole aligned. Due to the energetic position of the states within the band gap, indirect excitation through the conduction band will occur for sufficiently large excitation energies, leading to the misalignment of the absorptive and emissive dipoles seen in experiment. Our calculations predict a singlet ground state and the existence of a metastable triplet state, in agreement with experiment.

Hexagonal boron nitride (h-BN) displays numerous desirable properties, such as a wide band gap [1] and excellent stability [2]; thanks to advances in growth techniques [3], h-BN has been incorporated into electronic and optoelectronic devices [4]. Bright single-photon emission from point sources in h-BN has also recently been reported [5]. The emission features strong zero-phonon lines (ZPLs) in the visible spectrum with modest coupling to phonon modes [6], rendering these sources extremely attractive for applications in quantum information science. However, in spite of extensive experimental efforts, the microscopic origin of these single-photon emitters (SPEs) has not been identified.

It has been found that the SPEs with ZPLs ranging from 1.6 to 2.2 eV can be created with electron irradiation or with a high-temperature anneal [5], and ion implantation can be used to increase the formation probability of emitters [7]. Interestingly, h-BN samples grown with low pressure chemical vapor deposition (CVD) already have the emitters present, with ZPLs ranging from 2.10 to 2.18 eV [8]. Weak coupling to phonons is desirable for SPEs, since it concentrates intensity into a sharp zero-phonon line. The experimentally observed Huang-Rhys factor, a dimensionless parameter that characterizes the strength of electron-phonon coupling, is low for the SPEs in h-BN [6]. Furthermore, the emitters are linearly polarized [6, 7]. Some information about the spin state is also available: Exarhos *et al.* found that some emitters exhibit magnetic field dependence and suggested a singlet-to-triplet intersystem crossing model [9]. Coupling to magnetic fields is an important attribute since it enables spin qubits and spin-based sensing [10].

Theoretical studies have proposed a variety of different centers as potential candidates for the SPEs. Many of the proposals involved vacancies, for example V_N-C_B or V_N-N_B complexes [11–15]. However, the proposed centers have extremely high formation energies, making their observation in as-grown material highly unlikely.

Here we propose that dangling bonds (DBs) are the source of the observed single-photon emission in h-BN. DBs are different and distinct from the many other sources proposed to date, and exhibit properties in excellent agreement with experimental observations. DBs are formed when the regular bonding arrangement in a crystalline material is disrupted; they can be found at surfaces, interfaces, grain boundaries, and in voids. Experimental support for the attribution of SPEs to dangling-bond-like defects comes from the observation that emitters are typically localized near crystal edges or grain boundaries [7, 16, 17]. While DBs may be sensitive to their local environment, they can be extremely stable and plentiful, e.g. they are the primary defect in Si/SiO_2 interfaces [18].

To our knowledge, our present study is the first to examine DBs in h-BN. We will demonstrate that DBs act as single-photon emitters with characteristics that are consistent with experimental observations. This new view of DBs, as quantum defects with controllable properties, may be extended to other systems for which single-photon emission has been observed without attribution. In addition, the information generated here is also valuable in the context of using h-BN in electronic devices, since the presence of DBs can seriously impact device performance [19, 20].

In this Letter, we uncover the physics of DBs in h-BN through first-principles calculations. We focus on B DBs; we will show that N DBs do not possess the necessary level structure to give rise to 2-eV emission. It has been shown that h-BN flakes are predominantly N terminated [21–23]. Boron DBs will therefore be relatively rare (occurring, e.g., at corners or kinks [24]), in agreement with experimental observations. In the ground state, the B DB is doubly occupied. An internal transition can occur where one of the electrons is excited into a local-

ized p_z state on the B atom, as shown by the calculated configuration coordinate diagram in Fig. 1, which will be explained later. The properties of these transitions are in excellent agreement with the observed characteristics of the SPEs: luminescence occurs with a ZPL of 2.06 eV and a Huang-Rhys factor of 2.3. With regard to polarization, direct excitation into the p_z state leads to emissive dipoles aligned with absorption, but modest increases in the excitation energy lead to excitation into extended states and a consequent lack of dipole alignment, in good agreement with experimental observations of polarization [25]. The ground state of the doubly occupied B DB is a singlet, and the optical transitions described above are spin-conserving; however, we find that an intersystem crossing to a metastable triplet state exists [9]. All of these calculated properties indicate that doubly-occupied B DBs are the likely microscopic origin of the observed 2-eV SPEs.

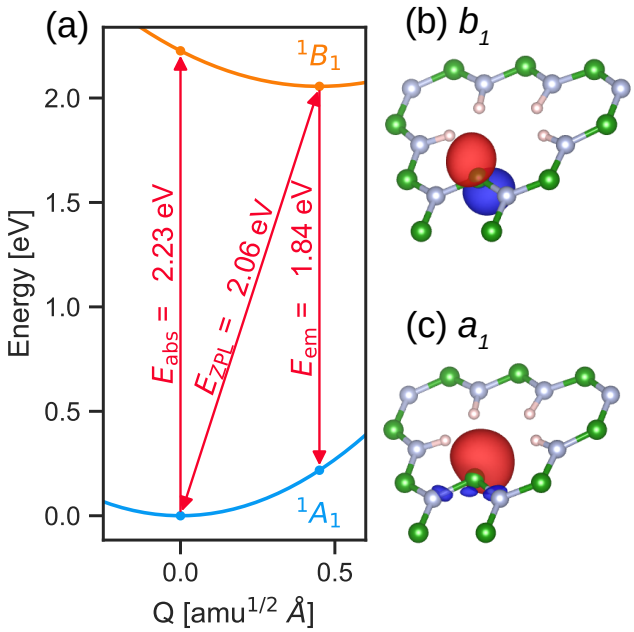

FIG. 1. (a) Calculated configuration coordinate diagram for the $^1A_1 \rightarrow {}^1B_1$ internal transition of the doubly occupied B DB. (b) Charge density isosurface of the B p_z state that becomes localized upon excitation. (c) Charge density isosurface of the B DB state that the electron occupies in the ground state. The isosurfaces correspond to 10% of the maximal charge density and are colored by the sign of the wavefunction, with red and blue indicating opposite signs.

Our calculations are based on hybrid density functional theory and projector augmented wave (PAW) potentials [26] as implemented in the VASP code [27]. The energy cutoff for the plane-wave basis set is 520 eV. We use the hybrid functional of Heyd, Scuseria, and Ernzerhof [28, 29] with the Grimme-D3 scheme to correct for the van der Waals interactions [30]. This approach has been extensively tested, both in the context of the present study and as part of previous work on h-BN [31, 32]. The fraction of non-local Hartree-Fock exchange α is set to 0.40; this results in a band gap of 6.41 eV which is consistent with the experimentally observed gap [1] when zero-point renormalization due to electron-phonon interactions [33, 34] is taken into account. This value of the mixing parameter is also close to satisfying the Koopmans condition [35]. The resulting lattice parameters are $a = 2.48$ Å and $c = 6.57$ Å, within 1.2% of the experimental values ($a = 2.50$ Å and $c = 6.65$ Å [36]). Defects are investigated in a 240-atom supercell, constructed by first building an orthorhombic cell ($a \times a\sqrt{3} \times c$) from two h-BN primitive cells and then scaling by $5 \times 3 \times 2$. The lattice vectors are held fixed, and atomic coordinates are relaxed until forces are below 0.01 eV/Å. Brillouin-zone sampling is performed using a single special $\mathbf{k}$ point $(1/4, 1/4, 1/4)$. Spin polarization is explicitly taken into account.

Removing a single host atom, i.e., forming a vacancy, creates three DBs; however, the close spacing of atoms surrounding the vacancy leads to strong interactions that significantly modify the electronic structure. As we will see, the properties of isolated DBs are very different from those of vacancy centers. To simulate the properties of an isolated DB, we employ the geometry of Ref. 37. For instance, to construct a B DB we remove a neighboring N atom, as well as two additional B atoms [see Fig. 2(a)]. This process creates a small void, containing the primary B DB that we wish to study, plus four secondary N DBs. In order to create a reference structure, all five DBs are passivated with hydrogen, and the atomic coordinates are relaxed allowing only in-plane degrees of freedom. In subsequent calculations, the B DB is studied by removing the hydrogen from the B-H bond, and relaxing atoms up to second-nearest neighbors, keeping all other atoms in the reference structure fixed. All relevant parameters are obtained as energy differences, in which the contributions from the fixed atoms in the reference structure cancel.

Equilibrium structures for the B and N DBs are shown in Fig. 2(a) and (b). Our calculations indicate that in this idealized geometry the DBs have C_{2v} symmetry with the two-fold rotation axis pointing in-plane, along the DB. We choose a coordinate system with $\mathbf{x}$ pointing along the C_{2v} symmetry axis and adopt a convention where the B_1 irreducible representation transforms like the vector $\mathbf{z}$ (out of plane), and B_2 transforms like $\mathbf{y}$ (in plane). DBs may be occupied with zero, one, or two electrons, which in our calculations correspond to a positive, neutral, and negative charge state. The relative energies of these charge states depend on the Fermi level, and the Fermi-level positions where the transitions between different charge states occur are the thermodynamic tran-

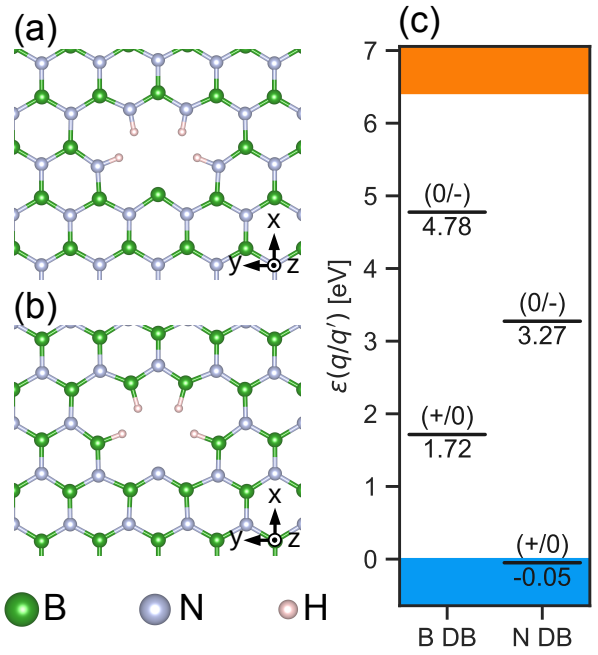

FIG. 2. Equilibrium structures for the (a) boron and (b) nitrogen DBs. Boron atoms are shown in green, nitrogen in gray, and hydrogen in white. (c) Calculated thermodynamic transition levels for both DBs. The valence and conduction band are highlighted in blue and orange.

sition levels [38]:

$$\epsilon(q/q') = \frac{1}{q'-q}[(E_{\rm tot}(q) + qE_{\rm VBM} + \Delta_q) - (E_{\rm tot}(q') + q'E_{\rm VBM} + \Delta_{q'})] \,, \quad (1)$$

where q and q' are the charges, $E_{\rm tot}$ is the total energy, and $E_{\rm VBM}$ is the energy of the valence-band maximum (VBM) from a bulk calculation. Δ_q is a charge-state-dependent correction that accounts for the finite size of the supercell [39, 40].

The computed thermodynamic levels for both the B and the N DBs are shown in Fig. 2(c). For the B DB, both the (+/0) and (0/−) thermodynamic levels are found within the band gap; therefore, the B DB may be unoccupied, singly occupied, or doubly occupied, depending on the Fermi-level position in the material. For the N DB, on the other hand, the (+/0) level is slightly below the VBM, indicating that the N DB will never be completely unoccupied in equilibrium. Kohn-Sham (KS) states for the two types of DBs are shown in Fig. 3. In the neutral charge state, the occupied KS state associated with the N DB is below the VBM. In the negative charge state, the N DB is fully occupied and has a_1 symmetry [Fig. 3(a)]; interestingly, a KS state with b_1 symmetry associated with the p_z state on the N atom has become localized and has moved into the band gap. No spin-conserving excitations to localized defect states can occur for either the singly or doubly-occupied N DB, and hence this DB cannot give rise to strong optical emission.

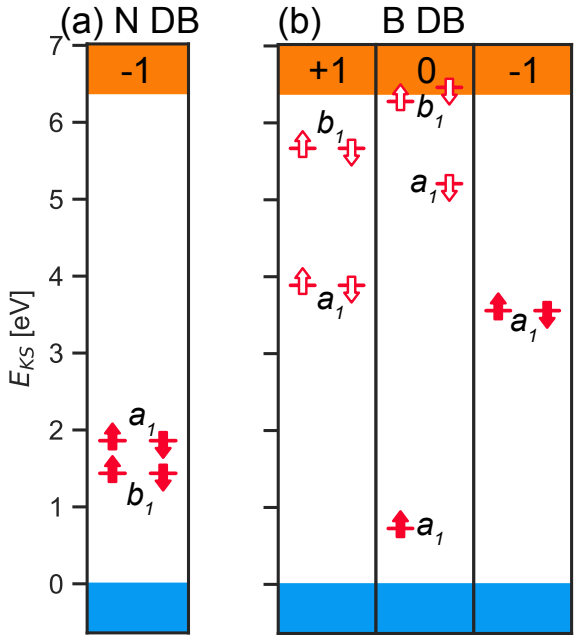

FIG. 3. Schematic depiction of the KS states for (a) the N DB in the negative charge state, and (b) the B DB in the positive, neutral, and negative charge states. The valence and conduction band are highlighted in blue and orange. Solid arrows depict occupied states, and open arrows depict unoccupied states.

The KS states for the B DB in all three charge states are shown in Fig. 3(b). In the positive charge state, the B DB is unoccupied, and KS states associated with the B p_z state (with b_1 symmetry) are also in the gap. Upon addition of one electron to the DB, the B p_z KS state shifts higher in energy and occupies a position just below the conduction-band minimum (CBM). Therefore, the neutral charge state of the B DB has the possibility of an internal transition, where the electron in the B DB can be excited into the B p_z state. In the negative charge state, two electrons occupy the DB; the B p_z state moves above the CBM and becomes delocalized. While this may seem to rule out the possibility of an internal transition, we will see that upon excitation (which leaves the a_1 state half occupied) the B p_z state becomes localized.

To study internal transitions we employ the ΔSCF methodology [41] in which excitation energies are computed as a total-energy difference between two calculations in which the occupations are constrained, each including full atomic relaxation. We employ configuration coordinate diagrams to schematically depict the coupling of these electronic transitions to lattice vibrations [10] and to compute the Huang-Rhys factors within the one-dimensional approximation [42]. The computed ZPL for the internal transition in the neutral charge state is 3.27

eV, with a Huang-Rhys factor of 7.9; this ZPL does not correspond to any observed single-photon emission.

In the negatively charged ground state, two electrons occupy the B DB in a singlet state, transforming like the A_1 irreducible representation of C_{2v}. We label the state $^1A_1$, where the superscript refers to the multiplicity $2S+1$ for a system of total spin S. We first consider the spin-conserving excitation of an electron from the DB to a B p_z state. The computed configuration coordinate diagram for this transition is shown in Fig. 1(a). Upon excitation the B p_z state becomes localized, transforming like the B_1 irreducible representation [shown in Fig. 1(b)]; we therefore label the excited state $^1B_1$. In the excited-state calculation, the KS state of the B p_z occurs just below the CBM, similar to the b_1 state in the neutral charge state. The ZPL for the $^1A_1 \rightarrow {}^1B_1$ transition is calculated to be 2.06 eV, in excellent agreement with the experimental reports [5, 8]. The Huang-Rhys factor for this transition is 2.3, on par with the range of experimental values reported in Ref. 6. The B DB is therefore a good candidate for the SPE, provided it occurs in a negative charge state, requiring the Fermi level to be sufficiently high in the band gap. Such a position is plausible, given the likelihood of oxygen contamination of the samples [43]. Oxygen impurities act as donors and drive the Fermi level towards the CBM [31].

One might expect that the emissive and absorptive dipoles would be aligned, but it has been reported that this is not necessarily the case [6]. Jungwirth and Fuchs [25] demonstrated that for resonant excitation the dipoles are aligned, but that misalignment occurs for higher excitation energies. The characteristics of B DBs nicely explain these observations. For excitations at or slightly above the resonant absorption energy [Fig. 1(a)], the alignment of the dipole is maintained. But because of the proximity of the b_1 state to the CBM, absorption at higher energy will place the electron in the conduction band, leading to a loss of polarization. The subsequent emission process, after the electron is captured into the excited state, then occurs with a polarization that is unrelated to the absorption dipole.

Our model of the negatively-charged B DB also predicts the presence of a metastable shelving state. The intersystem crossing to the shelving state is shown in Fig. 4. In addition to the $^1B_1$ excited state that occurs within the spin-singlet manifold, we can consider a $^3B_1$ triplet state where one electron occupies the DB and one occupies the B p_z state in a high-spin configuration. Our calculated level structure in Fig. 4 is similar to the singlet-to-triplet intersystem crossing proposed by Exarhos *et al.* [9] based on their study of the magnetic-field dependence of the SPEs, differing in the definition of B_1 and B_2 and the fact that they only considered diagrams with in-plane polarization.

Intersystem crossings depend on spin-orbit coupling to induce transitions. The spin-orbit coupling operator is given by $H_{SO} = \sum_i \boldsymbol{l}_i \cdot \boldsymbol{s}_i$, where i labels the electrons, $\boldsymbol{s}_i$ is the spin angular momentum operator, and the orbital angular momentum operator $\boldsymbol{l}_i$ is $(1/2m^2c^2)\boldsymbol{\nabla} V(\boldsymbol{r}_i) \times \boldsymbol{p}_j$, where V is the nuclear Coulomb potential [12]. Within C_{2v} symmetry, orbital angular momentum transforms like an axial vector with no A_1 component, and $B_1 \otimes B_1 = A_1$. Therefore, spin-orbit matrix elements between the $^1B_1$ and $^3B_1$ states are zero. In a lower symmetry, such as C_s, spin-orbit matrix elements between these states are non-zero and the intersystem crossing becomes allowed.

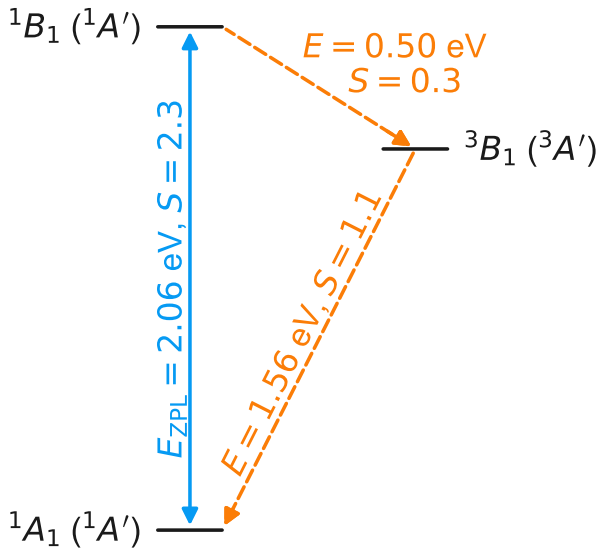

FIG. 4. Intersystem crossing of the doubly-occupied B DB. The solid blue line indicates an optical transition, and dashed orange lines indicate nonradiative crossings between spin channels. Alternative labels under C_s symmetry are given in parenthesis. Each transition is labeled with the transition energy and the Huang-Rhys factor S.

Indeed, such symmetry lowering should be expected for the dangling-bond defects proposed here. Given that these defects occur at the edge of flakes or near grain boundaries [7, 16, 17], the perfect C_{2v} symmetry as assumed in our idealized geometry will be broken. Local distortions and interactions will distort the DB out of plane and into a lower symmetry, such as C_s. This is in agreement with recent experiments that demonstrated Stark tuning of the SPEs in h-BN and suggested that an out-of-plane, permanent dipole is necessary to couple to the electric field [44]. The sensitivity of the properties of these DBs to the local environment explains why experimentally a range of SPEs with slightly different emission wavelengths are observed [5, 16, 17]. The identification of SPEs as DB defects actually allows us to propose an explanation for the mechanism by which nanopillars activate emitters in h-BN [45]: the induced curvature acts to bend the DBs out of plane.

Deviations from C_{2v} symmetry also account for the polarization of the optical transition. Selection rules

for electric dipole transitions would indicate that the ${}^1A_1 \rightarrow {}^1B_1$ transition is allowed only for out-of-plane polarization, while experiments report in-plane polarization [6, 7]. With C_s symmetry, both the ground and excited state orbitals will transform like A', and in-plane polarized transitions are allowed.

In summary, our calculations provide valuable information about the physics of DBs in h-BN. Doubly-occupied B DBs exhibit many of the experimentally reported features of single-photon emission. With a singlet ground state, an electron can be excited from the DB to a B p_z state; this internal transition has a ZPL at 2.06 eV. The calculated electronic structure of the DB explains why alignment of the absorptive and emissive dipoles depends on the excitation energy [25]. The dangling-bond system exhibits an intersystem crossing to a metastable triplet state, in agreement with experiment [9]. The sensitivity of DBs to the local environment explains why SPEs with a range of wavelengths have been observed [5, 16, 17], but offers exciting prospects for controlling and manipulating SPEs now that the microscopic origin has been identified.

We acknowledge fruitful discussions with M. Mackoit-Sinkevičienė. This work was supported by the National Science Foundation through the Materials Research Science and Engineering Centers (MRSEC) Program under Grant No. DMR-1720256 (Seed Program). L.C.B. acknowledges support from the Army Research Office (W911NF-15-1-0589). Computational resources were provided by the Extreme Science and Engineering Discovery Environment (XSEDE), supported by the NSF (ACI-1548562).

[1] G. Cassabois, P. Valvin, and B. Gil, Nat. Photonics **10**, 262 (2016).
[2] N. Kostoglou, K. Polychronopoulou, and C. Rebholz, Vacuum **112**, 42 (2015).
[3] Y. Kubota, K. Watanabe, O. Tsuda, and T. Taniguchi, Science **317**, 932 (2007).
[4] K. Watanabe, T. Taniguchi, T. Niiyama, K. Miya, and M. Taniguchi, Nat. Photonics **3**, 591 (2009).
[5] T. T. Tran, C. Elbadawi, D. Totonjian, C. J. Lobo, G. Grosso, H. Moon, D. R. Englund, M. J. Ford, I. Aharonovich, and M. Toth, ACS Nano **10**, 7331 (2016).
[6] A. L. Exarhos, D. A. Hopper, R. R. Grote, A. Alkauskas, and L. C. Bassett, ACS Nano **11**, 3328 (2017).
[7] S. Choi, T. T. Tran, C. Elbadawi, C. Lobo, X. Wang, S. Juodkazis, G. Seniutinas, M. Toth, and I. Aharonovich, ACS Appl. Mater. Interfaces **8**, 29642 (2016).
[8] N. Mendelson, Z.-Q. Xu, T. T. Tran, M. Kianinia, J. Scott, C. Bradac, I. Aharonovich, and M. Toth, ACS Nano (2019), 10.1021/acsnano.8b08511.
[9] A. L. Exarhos, D. A. Hopper, R. N. Patel, M. W. Doherty, and L. C. Bassett, Nature Communications **10**, 222 (2019).
[10] C. E. Dreyer, A. Alkauskas, J. L. Lyons, A. Janotti, and C. G. Van de Walle, Annu. Rev. Mater. Res. **48**, 1 (2018).
[11] S. A. Tawfik, S. Ali, M. Fronzi, M. Kianinia, T. T. Tran, C. Stampfl, I. Aharonovich, M. Toth, and M. J. Ford, Nanoscale **9**, 13575 (2017).
[12] M. Abdi, J.-P. Chou, A. Gali, and M. B. Plenio, ACS Photonics **5**, 1967 (2018).
[13] F. Wu, A. Galatas, R. Sundararaman, D. Rocca, and Y. Ping, Phys. Rev. Mater. **1**, 071001 (2017).
[14] A. Sajid, J. R. Reimers, and M. J. Ford, Phys. Rev. B **97**, 064101 (2018).
[15] G. D. Cheng, Y. G. Zhang, L. Yan, H. F. Huang, Q. Huang, Y. X. Song, Y. Chen, and Z. Tang, Comput. Mater. Sci. **129**, 247 (2017).
[16] Z.-Q. Xu, C. Elbadawi, T. T. Tran, M. Kianinia, X. Li, D. Liu, T. B. Hoffman, M. Nguyen, S. Kim, J. H. Edgar, X. Wu, L. Song, S. Ali, M. Ford, M. Toth, and I. Aharonovich, Nanoscale **10**, 7957 (2018).
[17] N. Chejanovsky, M. Rezai, F. Paolucci, Y. Kim, T. Rendler, W. Rouabeh, F. Fvaro de Oliveira, P. Herlinger, A. Denisenko, S. Yang, I. Gerhardt, A. Finkler, J. H. Smet, and J. Wrachtrup, Nano Lett. **16**, 7037 (2016).
[18] C. R. Helms and E. H. Poindexter, Rep. Prog. Phys. **57**, 791 (1994).
[19] J. R. Weber, A. Janotti, P. Rinke, and C. G. Van de Walle, Appl. Phys. Lett. **91**, 142101 (2007).
[20] M. Choi, A. Janotti, and C. G. Van de Walle, J. Appl. Phys. **113**, 044501 (2013).
[21] C. Jin, F. Lin, K. Suenaga, and S. Iijima, Phys. Rev. Lett. **102**, 195505 (2009).
[22] N. Alem, R. Erni, C. Kisielowski, M. D. Rossell, W. Gannett, and A. Zettl, Phys. Rev. B **80**, 155425 (2009).
[23] J. Kotakoski, C. H. Jin, O. Lehtinen, K. Suenaga, and A. V. Krasheninnikov, Phys. Rev. B **82**, 113404 (2010).
[24] F. Hayee, L. Yu, J. L. Zhang, C. J. Ciccarino, M. Nguyen, A. F. Marshall, I. Aharonovich, J. Vučković, P. Narang, T. F. Heinz, and J. A. Dionne, arXiv:1901.05952 [cond-mat] (2019).
[25] N. R. Jungwirth and G. D. Fuchs, Phys. Rev. Lett. **119**, 057401 (2017).
[26] P. E. Blöchl, Phys. Rev. B **50**, 17953 (1994).
[27] G. Kresse and J. Furthmüller, Phys. Rev. B **54**, 11169 (1996).
[28] J. Heyd, G. E. Scuseria, and M. Ernzerhof, J. Chem. Phys. **118**, 8207 (2003).
[29] J. Heyd, G. E. Scuseria, and M. Ernzerhof, J. Chem. Phys. **124**, 219906 (2006).
[30] S. Grimme, J. Antony, S. Ehrlich, and H. Krieg, J. Chem. Phys. **132**, 154104 (2010).
[31] L. Weston, D. Wickramaratne, M. Mackoit, A. Alkauskas, and C. G. Van de Walle, Phys. Rev. B **97**, 214104 (2018).
[32] D. Wickramaratne, L. Weston, and C. G. Van de Walle, J. Phys. Chem. C **122**, 25524 (2018).
[33] G. Antonius, S. Poncé, E. Lantagne-Hurtubise, G. Auclair, X. Gonze, and M. Côté, Phys. Rev. B **92**, 085137 (2015).
[34] R. Tutchton, C. Marchbanks, and Z. Wu, Phys. Rev. B **97**, 205104 (2018).
[35] G. Miceli, W. Chen, I. Reshetnyak, and A. Pasquarello, Phys. Rev. B **97**, 121112(R) (2018).
[36] Y. Gu, M. Zheng, Y. Liu, and Z. Xu, J. Am. Ceram.

Soc. **90**, 1589 (2007).
[37] C. G. Van de Walle and R. A. Street, Phys. Rev. B **49**, 14766 (1994).
[38] C. Freysoldt, B. Grabowski, T. Hickel, J. Neugebauer, G. Kresse, A. Janotti, and C. G. Van de Walle, Rev. Mod. Phys. **86**, 253 (2014).
[39] C. Freysoldt, J. Neugebauer, and C. G. V. d. Walle, Phys. Status Solidi B **248**, 1067 (2011).
[40] C. Freysoldt, J. Neugebauer, and C. G. Van de Walle, Phys. Rev. Lett. **102**, 016402 (2009).
[41] R. O. Jones and O. Gunnarsson, Rev. Mod. Phys. **61**, 689 (1989).
[42] A. Alkauskas, J. L. Lyons, D. Steiauf, and C. G. Van de Walle, Phys. Rev. Lett. **109**, 267401 (2012).
[43] T. Taniguchi and K. Watanabe, J. Cryst. Growth **303**, 525 (2007).
[44] G. Noh, D. Choi, J.-H. Kim, D.-G. Im, Y.-H. Kim, H. Seo, and J. Lee, Nano Lett. **18**, 4710 (2018).
[45] N. V. Proscia, Z. Shotan, H. Jayakumar, P. Reddy, C. Cohen, M. Dollar, A. Alkauskas, M. Doherty, C. A. Meriles, and V. M. Menon, Optica **5**, 1128 (2018).